

## Temperature dependence of tunneling magnetoresistance in epitaxial magnetic tunnel junctions using a Co<sub>2</sub>FeAl Heusler alloy electrode

Wenhong Wang,<sup>1,2</sup> Hiroaki Sukegawa,<sup>1</sup> and Koichiro Inomata<sup>1</sup>

<sup>1</sup>Magnetic Material Center, National Institute for Materials Science (NIMS), 1-2-1 Sengen, Tsukuba 305-0047, Japan

<sup>2</sup>Beijing National Laboratory for Condensed Matter Physics, Institute of Physics, Chinese Academy of Sciences, Beijing 100080, People's Republic of China

(Received 12 June 2010; published 20 September 2010)

Spin-valve-type epitaxial magnetic tunnel junctions (MTJs) consisting of a full-Heusler alloy Co<sub>2</sub>FeAl (CFA) and a MgO tunnel barrier were fabricated on a single-crystal MgO(001) substrate using sputtering method for all the layers. Experimental temperature-dependent tunnel magnetoresistance in the MTJs was revealed to be fitted well using spin wave excitation model for tunneling spin polarization,  $P(T)=P_0(1-\alpha T^{3/2})$  up to room temperature, where  $P_0$  is the spin polarization at 0 K and  $\alpha$  is a fitting parameter. The determined  $P$  and  $\alpha$  are shown to be significantly different between bottom and top CFA electrodes facing a MgO barrier. It is demonstrated that the bottom CFA deposited on a Cr buffer has a low  $\alpha$  and behaves as a half-metal with  $P\sim 1$  in terms of the  $\Delta_1$  symmetry due to the coherent tunneling through a MgO barrier.

DOI: 10.1103/PhysRevB.82.092402

PACS number(s): 85.75.-d, 75.47.-m, 73.20.At, 75.50.Cc

Most of Co-based full-Heusler alloys with a chemical form of Co<sub>2</sub>YZ ( $Y$ : transition metal,  $Z$ : main group element) have been predicted to be half-metallic ferromagnets, accompanied with high Curie temperatures ( $T_c$ ).<sup>1-3</sup> After the first experimental observation of tunnel magnetoresistance (TMR) at room temperature (RT) in a magnetic tunnel junction (MTJ) using Co<sub>2</sub>Cr<sub>0.6</sub>Fe<sub>0.4</sub>Al (CCFA) Heusler alloy electrodes,<sup>4</sup> the large TMR has been reported in MTJs using half-metallic Co-based full-Heusler alloy electrodes such as CCFA,<sup>5</sup> Co<sub>2</sub>FeAl<sub>0.5</sub>Si<sub>0.5</sub> (CFAS),<sup>6-11</sup> and Co<sub>2</sub>MnSi (CMS).<sup>12-16</sup> In general, however, TMR in MTJs using half-metallic full-Heusler alloy electrodes largely decreases with increasing temperature, especially for CMS electrode, of which origin has not been understood enough. The rapid reduction in TMR with temperature in CMS-based MTJs has been attributed to the Fermi level  $E_F$  near the bottom edge of the conduction band of CMS,<sup>12</sup> nonquasiparticle states appearing just above  $E_F$ ,<sup>17</sup> and the creation of interface states at  $E_F$  within the half-metallic gap of the half-metal/barrier interface and the spin-flipping process through the interface states mediated by magnon excitation.<sup>18</sup> On the other hand, nevertheless CFAS has  $E_F$  at the middle of the half-metallic band gap,<sup>10,11</sup> sputter-deposited MTJs with CFAS electrodes and a MgO barrier still show a large temperature dependence of TMR, although the degree of the reduction is not severe as in CMS-based MTJs, resulting in the maximum TMR ratio of 220% at RT and over 700% at a low temperature.<sup>7</sup> Higher TMR ratio of 386% at RT (832% at 9K) was reported in a CFAS/MgO/CFAS MTJ grown on a MgO(100) substrate using molecular beam epitaxy deposition techniques,<sup>19</sup> which also displays the large temperature-dependent TMR. Recently, we have demonstrated that the temperature dependence of TMR in epitaxial MTJs using a CFAS electrode and a MgAl<sub>2</sub>O<sub>4</sub> barrier with spinel structure can be explained quantitatively using Julliere's model for TMR [ $\text{TMR ratio} = 2P_1P_2/(1-P_1P_2)$ ] (Ref. 20) and the spin wave excitation model for the spin polarization  $P(T)=P_0(1-\alpha T^{3/2})$ , where  $P_0$  is the spin polarization at 0 K and  $\alpha$  is a constant dependent on magnetic materials for electrodes and the interface

structure.<sup>11</sup> We pointed out in the study that the spin-independent contribution to the tunneling is negligibly small in the epitaxial MTJs and  $\alpha$  is larger at the interface between half-metallic electrode and a barrier than that of the bulk due to the larger thermal fluctuation of the magnetization at the interface than that of the bulk, which leads to a large temperature dependence of the TMR. Thus the temperature dependence of the TMR may be sensitive to the interface structure as well as  $T_c$  of the electrodes. Very recently, we have succeeded to achieve a large TMR ratio of 330% at RT and 700% at 10 K with an improved temperature dependence of TMR in an epitaxial Co<sub>2</sub>FeAl (CFA)/MgO/CoFe/IrMn MTJ fabricated using sputter-deposition techniques for all the layers, where CFA is deposited on a Cr-buffered MgO(100) substrate and has  $B2$  structure.<sup>21</sup> This large TMR was attributed to the coherent tunneling effect<sup>22,23</sup> because  $B2$ -CFA is not a half-metal.<sup>24,25</sup>

In the present Brief Report, we analyze the temperature dependence of TMR measured for various epitaxial MTJs with a MgO barrier using CFA as an electrode and show that the temperature dependence of TMR can be fitted well using Julliere's model for TMR and the spin wave excitation model for the tunneling spin polarization ( $P$ ) as in the case of CFAS-based MTJs.<sup>11</sup> We found that both the interfacial morphology and the quality are critical for maintaining the high  $P$  values of the electrodes and coherent tunneling effect, which are actually rather lost in the discussion of Julliere's model. It is further demonstrated that the  $P$  values are significantly different between two electrodes facing a MgO barrier; a top electrode on a MgO barrier has significantly smaller  $P$  and larger  $\alpha$  than those of a bottom electrode underneath the barrier, which indicates that the quality of top interface is difficult to maintain but also critical. The analysis exhibits that the bottom CFA has almost  $P\sim 1$  and a small  $\alpha$  of  $0.75\times 10^{-5}$  while top CFA has  $P=0.68$  and  $\alpha=3.54\times 10^{-5}$ .

The MTJs with a structure of CFA(30)/MgO(1.8)/CFA(5)/Ir<sub>80</sub>Mn<sub>20</sub>(12)/Ru(7) (unit: nm) was fabricated on a Cr(40)- or MgO(10)-buffered MgO(001) substrate using an

ultrahigh vacuum magnetron sputtering system with the base pressure of below  $8 \times 10^{-8}$  Pa. CFA(30)/MgO(1.8)/CoFe(5)/Ir<sub>80</sub>Mn<sub>20</sub>(12)/Ru(7) MTJ was also fabricated on a Cr(40)-buffered MgO(001) substrate, where CoFe means Co<sub>75</sub>Fe<sub>25</sub>. The bottom CFA electrode was deposited at RT from a stoichiometric Co-Fe-Al (Co: 50.0%, Fe: 25.0%, Al: 25.0%) target. The Ar pressure during sputtering was 1.0 mTorr and typical deposition rate was  $2 \times 10^{-2}$  nm/s for CFA. We found that the as-deposited CFA film composition was Co<sub>52.8</sub>Fe<sub>25.4</sub>Al<sub>21.8</sub> through inductively coupled plasma analysis. The film was subsequently annealed at 480 °C for 15 min in order to improve the quality. The crystal structures were characterized by x-ray diffraction (XRD). Surface morphology and surface roughness were investigated using atomic force microscopy (AFM). The MgO tunnel barrier was formed by rf sputtering directly from a sintered MgO target under an Ar pressure of 10 mTorr. The MTJs were patterned into an area of  $10 \times 10 \mu\text{m}^2$  using conventional photolithography and Ar ion milling process. Patterned MTJs were annealed at  $T_a$  from 300 to 475 °C for 1 h in high vacuum by applying a 5 kOe magnetic field. Magnetoresistance measurements were carried out using the standard dc four-point probe method from 7 to 300 K. In this study, magnetic field was applied along in the plane and the positive voltage is defined as that electrons flow from the top layer to the bottom layer.

XRD indicated that the CFA film deposited at RT and subsequently annealed at 480 °C grows with *B2* structure and almost perfect (001) orientation on both Cr- and MgO-buffered MgO(001) surfaces, which implies the existence of complete disorder between Fe and Al, while Co atoms occupy regular sites. The surface morphology observed by AFM was extremely flat and an average surface roughness (*Ra*) of 0.2 nm was achieved for the 480 °C-annealed CFA film. Fig. 1(a) shows the typical TMR curves for three different MTJs consisting of CFA/MgO/CoFe and CFA/MgO/CFA, deposited on a Cr-buffered MgO(100) substrate, respectively, and CoFe/MgO/CoFe deposited on a MgO-buffered MgO(100) substrate as a reference. All the MTJs are epitaxially grown and exchange biased using an IrMn antiferromagnet. The maximum TMR ratio is 330%, 223%, and 140% for CFA/MgO/CoFe, CFA/MgO/CFA, and CoFe/MgO/CoFe MTJs, respectively. Figure 1(b) shows the temperature dependence of TMR for three different MTJs. The TMR ratio increased as the temperature is reduced attaining a value of 700%, 415%, and 268% at 10 K for CFA/MgO/CoFe, CFA/MgO/CFA, and CoFe/MgO/CoFe MTJs, respectively. The comparison between CFA/MgO/CoFe and CoFe/MgO/CoFe MTJ suggests that CFA has much larger *P* than that of CoFe. However, the TMR in CFA/MgO/CFA MTJ is significantly smaller than that in CFA/MgO/CoFe MTJ in contradiction to the prediction of higher *P* for CFA than CoFe. This apparent inconsistency can be understood by considering different *P* values between the bottom and top CFA electrodes facing an MgO barrier due to the different interface structures. In fact we have obtained higher TMR of 785% and 360% at 10 K and RT, respectively for a Cr/CFA/MgO/CoFe(0.5)/CFA MTJ with 0.5-nm-thick CoFe insertion between MgO barrier and top CFA, which improves the CFA interface.

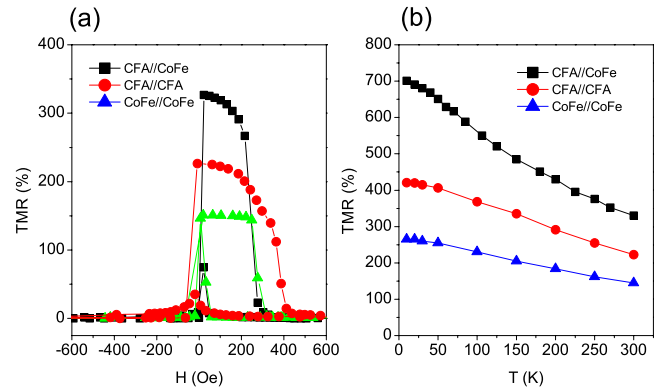


FIG. 1. (Color online) (a) Representative TMR curves for exchange biased MTJs consisting of CFA/MgO/CoFe and CFA/MgO/CFA, deposited on a Cr-buffered MgO(100) substrate, respectively, and CoFe/MgO/CoFe deposited on a MgO-buffered MgO(100) substrate as a reference, where CFA means Co<sub>2</sub>FeAl and MgO thickness  $t_{\text{MgO}}=1.8$  nm. The maximum TMR ratio is 330%, 223%, and 140% for CFA/MgO/CoFe, CFA/MgO/CFA, and CoFe/MgO/CoFe MTJs, respectively. (b) Plots of detailed evolution of TMR ratio versus temperature for the three MTJs. The TMR ratios increase as the temperature is reduced attaining a value of 700%, 415%, and 268% at 10 K for CFA/MgO/CoFe, CFA/MgO/CFA, and CoFe/MgO/CoFe MTJs, respectively. All measurements were conducted at RT under an applied bias voltage of +1 mV.

In order to clarify the different *P* values between the bottom and top electrodes we have analyzed the temperature dependence of TMR using Julliere's model for TMR ratio and spin wave excitation model for *P* of electrodes in the MTJs. We have neglected the spin-independent contribution to the tunneling as in Ref. 11 and assumed  $P_0$  to be the same as the value at 10 K. An excellent fitting curve for the temperature dependence of TMR in CoFe/MgO/CoFe MTJ was obtained using  $P_0=0.76$  and  $\alpha=3.2 \times 10^{-5}$  for both CoFe, assuming the same *P* and  $\alpha$  for top and bottom CoFe electrodes facing an MgO barrier. By using these values for CoFe we successfully fitted the experimental result for Cr/CFA/MgO/CoFe MTJ as shown with a solid line in Fig. 2(a), which gives  $P_0=0.99$  and  $\alpha=7.5 \times 10^{-6}$  for the bottom CFA on a Cr buffer. It is noticeable that the  $P_0$  value implies almost half-metallicity of the bottom CFA on a Cr buffer due to the coherent tunneling effect. This is consistent with the calculated band dispersion of *B2*-CFA along [001] direction, in which  $\Delta_1$  band exists for the majority spin but not for the minority spin at  $E_F$ .<sup>22</sup> The small  $\alpha=7.5 \times 10^{-6}$  may be originated from the very flat interface between the bottom CFA and a MgO barrier.<sup>21</sup> The small  $\alpha$  of  $7.5 \times 10^{-6}$  and the large  $P_0$  of 0.99 bring a very large tunneling spin polarization at RT,  $P$  (RT)=0.96 for Cr/CFA/MgO structure.

The temperature-dependent TMR in Cr/CFA/MgO/CFA MTJ can also be fitted well using the same values of *P* and  $\alpha$  estimated for bottom CFA as shown in Fig. 2(b), which leads to  $P_0=0.68$  and  $\alpha=3.5 \times 10^{-5}$  for the MgO barrier/top CFA structure. The *P* and  $\alpha$  of the top CFA on a MgO barrier are significantly smaller and larger compared with those of the bottom CFA, respectively, although the  $\alpha$  is comparable to the value of CoFe, suggesting that the top CFA on a MgO barrier has a degraded interface with disordered structure and

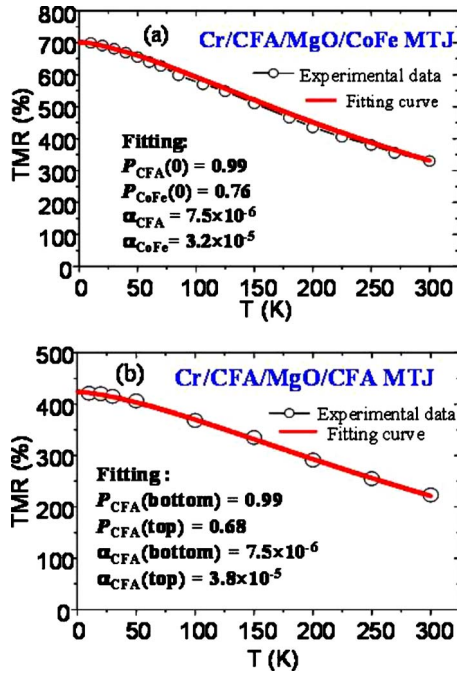


FIG. 2. (Color online) Fitting of the temperature dependence of TMR using Julliere’s model for TMR ratio and spin wave excitation model for tunneling spin polarization  $P$  for (a) Cr/CFA/MgO/CoFe and (b) Cr/CFA/MgO/CFA MTJs (solid red lines). Open circles are experimental data.

larger roughness compared with the bottom interface due to the thinner MgO barrier and top CFA thicknesses. Bottom CFA on a Cr buffer is *in situ* annealed at 480 °C before depositing an MgO barrier, which provides highly  $B2$ -ordered and better interface of the bottom CFA. The comparable  $\alpha$  between top CFA and CoFe may be based on nearly the same magnitude of  $T_c$  and similar top interface structure with each other.

By applying  $P_0=0.76$  and  $\alpha=3.2 \times 10^{-5}$  for CoFe to an exchange-biased MgO buffer(20)/CFA(30)/MgO(1.8)/

TABLE I. The values of  $P$  and  $\alpha$  estimated above for CFA and CoFe on different buffers and an MgO barrier. The  $b$  and  $t$  mean bottom and top layers with respect to the MgO barrier, respectively.

	$P$		
	10 K	RT	$\alpha(\times 10^{-5})$
Cr buffer/CFA/MgO	0.990	0.960	0.75 ( <i>b</i> -CFA)
MgO buffer/CFA/MgO	0.902	0.867	0.75 ( <i>b</i> -CFA)
MgO/ <i>t</i> -CFA	0.680	0.551	3.54 ( <i>t</i> -CFA)
MgO buffer/CoFe/MgO	0.753	0.628	3.2 ( <i>b</i> -CoFe)
MgO/ <i>t</i> -CoFe	0.760	0.634	3.2 ( <i>t</i> -CoFe)

CoFe(5)/IrMn(10)/Ru MTJ fabricated, we have succeeded to fit well the temperature dependence of TMR for the MTJ using  $P_0=0.90$  and  $\alpha=0.75 \times 10^{-6}$  for bottom CFA on a MgO buffer. The  $P_0=0.90$  is slightly lower than 0.99 of the CFA on a Cr buffer. This may be caused by the difference of the disordering in CFA between on a Cr buffer and an MgO buffer, which was revealed by  $^{59}\text{Co}$  NMR measurements.<sup>24</sup> The values of  $P_0$  and  $\alpha$  estimated above are listed in Table I for CFA and CoFe on different buffers and a MgO barrier. The significantly small  $P_0$  of CFA on a MgO barrier (0.68) compared with that on a MgO buffer (0.90) suggests the interface and bulk structure differences of CFA between on the barrier and buffer because MgO barrier thickness (1.8 nm) is much thinner than that of the MgO buffer (20 nm). The structure of CFA on a thin MgO barrier may be more disordered at the interface and the bulk. We can calculate TMR ratio for MgO buffer/CFA/MgO/CFA MTJ using  $P_0$  and  $\alpha$  estimated for top and bottom CFA, which provides 310% and 183% at a low temperature and RT, respectively. The 183% at RT is in excellent agreement with the experimentally obtained TMR of 188% at RT.<sup>26</sup> This result indicates that the  $P_0$  and  $\alpha$  values listed in Table I for bottom and top electrodes facing an MgO barrier are acceptable.

The tunneling mechanism based on the coherent tunneling

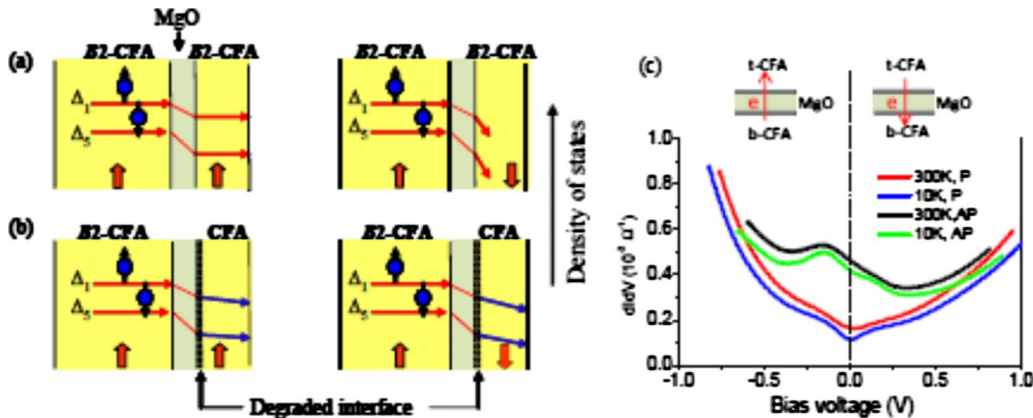


FIG. 3. (Color online) Schematic tunneling mechanism based on the coherent tunneling effect for Cr/CFA/MgO/CFA MTJs with perfect (a) and disordered (b) interfaces between MgO barrier and top CFA, where the bottom interface is assumed to be perfect. Interface wave function matching and tunneling probability for the disordered top interface (b) are changed, which leads to TMR reduction. (c) Bias voltage dependence of differential tunneling conductance  $dI/dV$ - $V$  curves at 300 and 10 K for CFA/MgO/CFA MTJ. Asymmetric bias-dependence curves were observed, despite the symmetric CFA/MgO/CFA films structure. Here a negative bias voltage means that electrons are tunneling from bottom electrode to top electrode; P and AP stand for parallel and antiparallel alignment of the two electrodes.



effect is illustrated schematically in Fig. 3 for Cr/CFA/MgO/CFA MTJs with perfect (a) and disordered (b) interfaces between MgO barrier and top CFA, where the bottom interface is assumed to be perfect because we have obtained  $P_0 \sim 1$  for Cr/CFA/MgO barrier structure. The changes of interface wave function matching and tunneling probability for the disordered interface will decrease and increase  $\Delta_1$  and  $\Delta_5$  band contributions to tunneling in (a) and (b), respectively, resulting in the TMR reduction and the reduced tunneling spin polarization. This interpretation remains in agreement with the results of Fig. 3(c) which show the dependences of differential conductance ( $G=dI/dV$ ) of CFA/MgO/CFA MTJ. We found that the conductance characteristics of the MTJ exhibit a strongly asymmetry regarding the polarity and a pronounced dip in the positive bias direction, which differs considerably from those of the CFA/MgO/CoFe MTJs as in Ref. 24. Basically,  $G_P$  ( $V$ ) mainly reflects the character of the electronic structure of the electrode where electrons flow out. Here a positive bias voltage means that electrons are tunneling from top electrode to bottom electrode. Therefore, the strong decrease of  $G_P$  curve in the positive bias suggests the structural quality of the upper-MgO/CFA interface is reduced with respect to the lower one. If could realize the same interface for MgO barrier/top CFA as that of the MgO buffer/CFA with  $P_0=0.9$ , the TMR of 1800% at RT is predicted to be achieved for a Cr/CFA/MgO/CFA MTJ, since bottom CFA has  $P_0 \sim 1$  and both CFA electrodes have  $\alpha=0.75 \times 10^{-6}$ . This will be a challenging issue.

Finally resistance ( $R$ ) $\times$ area( $A$ ) product dependence of TMR at RT with different MgO barrier thicknesses  $t_{\text{MgO}}$  is shown in Fig. 4 for Cr(40)/CFA(30)/MgO( $t_{\text{MgO}}$ )/CoFe(5)/IrMn(10)/Ru MTJs. The TMR for  $t_{\text{CFA}}=2.5$  nm is also plotted for a MTJ with  $t_{\text{MgO}}=0.8$  nm. The TMR decreases with decreasing MgO thickness in accordance with a feature of coherent tunneling effect. Surprisingly, however, TMR keeps over 100% at RT for  $\text{RA}=5 \Omega \mu\text{m}^2$  and even for  $t_{\text{CFA}}=2.5$  nm. This large TMR may be caused by that the coherent tunneling effect works effectively for a MTJ with small RA and thin CFA thickness, which may be due to the good interface structure between bottom CFA and an MgO

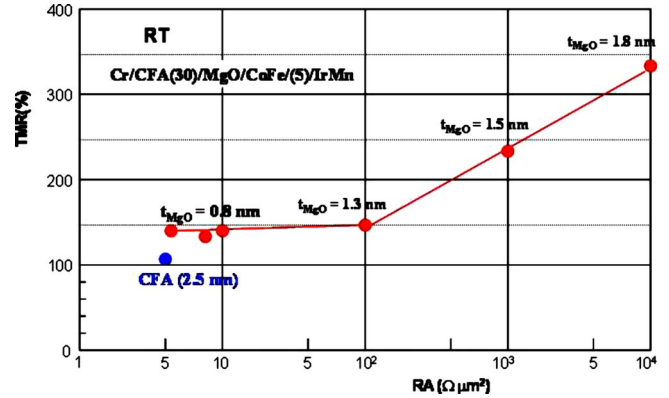


FIG. 4. (Color online) TMR ratio at RT as a function of resistance ( $R$ ) $\times$ area( $A$ ) product for Cr(40)/CFA(30)/MgO( $t_{\text{MgO}}$ )/CoFe(5)/IrMn(10)/Ru MTJs with different MgO barrier thicknesses.

barrier. MTJs with a thin free layer accompanied with a large TMR and a small RA are indispensable for magnetization switching by spin transfer torque which is a key technology in high density MRAMs and spin logic etc. Thus, CFA will be a promising material for practical applications in spintronics.

In summary, we have investigated the temperature dependence of TMR in fully epitaxial MTJs with a  $B2$ -ordered CFA electrode and an MgO tunnel barrier on a MgO(001) substrate fabricated using simple sputter-deposition techniques. Temperature-dependent TMR was demonstrated to be fitted well using Julliere's model for TMR and spin wave excitation model for  $P$ . The obtained  $P$  and  $\alpha$  are significantly different between bottom and top CFA facing a MgO barrier, where the bottom CFA deposited on a Cr buffer has  $P_0 \sim 1$  and  $\alpha=0.75 \times 10^{-5}$  while the top CFA on a MgO barrier has  $P_0 \sim 0.68$  and  $\alpha=3.5 \times 10^{-5}$ . This difference is attributed to the differences of the interface structure and disordering structure in the bulk between bottom and top CFA.

This work was partly supported by the NEDO, CREST, and JST-DFG.

<sup>1</sup>S. Ishida *et al.*, *J. Phys. Soc. Jpn.* **64**, 2152 (1995).

<sup>2</sup>I. Galanakis *et al.*, *Phys. Rev. B* **66**, 174429 (2002).

<sup>3</sup>C. Felser (unpublished).

<sup>4</sup>K. Inomata *et al.*, *Jpn. J. Appl. Phys., Part 2* **42**, L419 (2003).

<sup>5</sup>T. Marukame *et al.*, *Appl. Phys. Lett.* **90**, 012508 (2007).

<sup>6</sup>N. Tezuka *et al.*, *Appl. Phys. Lett.* **89**, 252508 (2006).

<sup>7</sup>N. Tezuka *et al.*, *Jpn. J. Appl. Phys., Part 2* **46**, L454 (2007).

<sup>8</sup>K. Inomata *et al.*, *Sci. Technol. Adv. Mater.* **9**, 014101 (2008).

<sup>9</sup>W. H. Wang *et al.*, *Appl. Phys. Lett.* **92**, 221912 (2008).

<sup>10</sup>H. Sukegawa *et al.*, *Phys. Rev. B* **79**, 184418 (2009).

<sup>11</sup>R. Shan *et al.*, *Phys. Rev. Lett.* **102**, 246601 (2009).

<sup>12</sup>Y. Sakuraba *et al.*, *Appl. Phys. Lett.* **88**, 022503 (2006).

<sup>13</sup>Y. Sakuraba *et al.*, *Appl. Phys. Lett.* **89**, 052508 (2006).

<sup>14</sup>S. Tsunegi *et al.*, *Appl. Phys. Lett.* **93**, 112506 (2008).

<sup>15</sup>T. Ishikawa *et al.*, *Appl. Phys. Lett.* **89**, 192505 (2006).

<sup>16</sup>T. Ishikawa *et al.*, *J. Appl. Phys.* **103**, 07A919 (2008).

<sup>17</sup>L. Chioncel *et al.*, *Phys. Rev. Lett.* **100**, 086402 (2008).

<sup>18</sup>P. Mavropoulos *et al.*, *Phys. Rev. B* **72**, 174428 (2005).

<sup>19</sup>N. Tezuka *et al.*, *Appl. Phys. Lett.* **94**, 162504 (2009).

<sup>20</sup>M. Julliere, *Phys. Lett.* **54A**, 225 (1975).

<sup>21</sup>W. H. Wang *et al.*, *Appl. Phys. Lett.* **95**, 182502 (2009).

<sup>22</sup>W. H. Butler *et al.*, *Phys. Rev. B* **63**, 054416 (2001).

<sup>23</sup>J. Mathon and A. Umerski, *Phys. Rev. B* **63**, 220403(R) (2001).

<sup>24</sup>W. H. Wang *et al.*, *Phys. Rev. B* **81**, 140402(R) (2010).

<sup>25</sup>T. M. Nakatani *et al.*, *J. Appl. Phys.* **102**, 033916 (2007).

<sup>26</sup>Experimentally, we found the TMR ratios of MgO buffer/CFA/MgO/CoFe and MgO buffer/CFA/MgO/CFA MTJs are 244% and 188% at RT, respectively.